Influence of the Continuous and Dispersed Phases on the Symmetry of a Gas Turbine Air-Blast Atomizer

V. G. McDonell

G. S. Samuelsen

UCI Combustion Laboratory,
UCI Institute for Combustion and
Propulsion Sciences and Technology,
University of California, Irvine,
Irvine, CA 92717

Current trends in liquid-fueled practical combustion systems are leaving less tolerance for fuel injection deficiencies such as poor spray field symmetry. The present paper evaluates the symmetry of the flowfield produced by a practical air-blast atomizer. Specifically, the influence of both the continuous phase and dispersed phase on the spray field symmetry is assessed. In the present case, asymmetry in volume flux is associated principally with disparities in the injection of the dispersed phase, which is manifested by a maldistribution of larger drops. Asymmetries observed in the continuous phase without the dispersed phase are reduced in magnitude by the presence of the dispersed phase, but still contribute to asymmetry in radial spread of the dispersed phase.

Introduction

The need to assess spray field symmetry in liquid-fueled combustion systems is gaining importance for several reasons. First, the move to fuel flexible systems and smaller geometries leaves less tolerance for local variation in combustor performance due to atomizer asymmetry. Second, the current development of numerical codes for liquid-fueled systems is predicated on the assumption of spray field symmetry. Third, the measurement of droplet size and velocity typically assumes spray symmetry with the concomitant acquisition of data along a single radius rather than a full diameter. The interpretation of such data is jeopardized in the absence of atomizer symmetry.

The spray fields produced by air-assist or air-blast atomizers are a result of considerable two-phase interaction. Therefore, it is important to assess the role of *each phase* in order to understand the generation of any asymmetry present. Recently introduced modern diagnostics, coupled with conventional methods, portend the capability of providing the needed assessment of symmetry of the dispersed phase in both isothermal and combustor environments. Recent results have demonstrated the potential of these modern diagnostics in both environments (e.g., McDonell et al., 1987).

The objective of the research reported in the present paper is to explore the extent to which the dispersed *and* continuous phases contribute to the symmetry of an air-blast atomizer using modern methods in an isothermal environment. This study provides a baseline against which the performance of the same atomizer under reacting conditions may be compared.

Contributed by the International Gas Turbine Institute and presented at the 34th International Gas Turbine and Aeroengine Congress and Exhibition, Toronto, Ontario, Canada, June 4-8, 1989. Manuscript received at ASME Headquarters February 21, 1989. Paper No. 89-GT-303.

Experiment

Atomizer. The atomizer selected for characterization, shown in Fig. 1, is a production air-blast atomizer for use in a production helicopter gas turbine engine (Mongia and Reider, 1985). The atomizer features swirled, centrally injected air and, via an outer shroud, swirling external air. The fuel is filmed onto a circular surface (via six ports, which inject the fuel tangentially in the same direction as the swirled air) and sheared between the two air passages.

Methanol is the liquid fuel used in the present study. It was selected due to suitability of the resultant data for modeling. In particular, the methanol vapor has nearly the same density as air (1.33 versus 1.2 kg/m^3) and, when injected at $-10°C$ ($-10°C$ is the wet bulb temperature at test conditions), evaporates isothermally and thereby eliminates density gradients in the gaseous environment and temperature gradients within the droplets. The atomizer is operated at an air-to-fuel ratio of 1.0 and a mass flow of 0.0021 kg/s for each phase. The pressure drops across the atomizer are 5600 Pa and 125 Pa for the fuel and air, respectively.

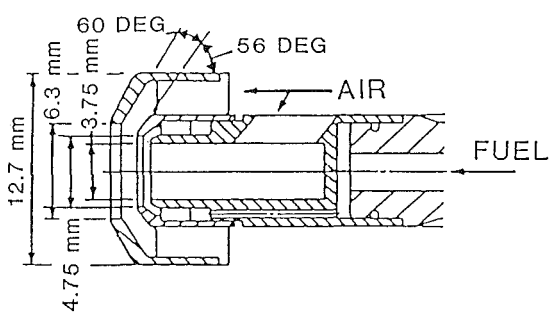

Fig. 1 Fuel injector

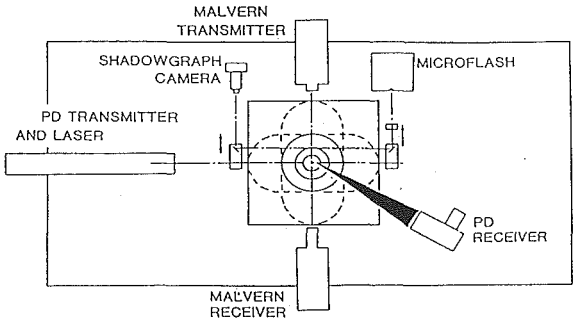

Fig. 2 Facility

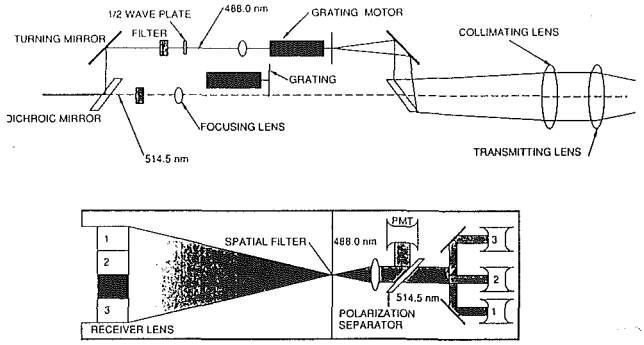

Fig. 3 Two-component phase Doppler transmitter and receiver

Spray Characterization Facility. A schematic of the test facility is shown in Fig. 2. The diagnostics remain fixed, oriented about a square cutout in the optical table that measures 900 × 900 mm. The test article is directed downward from the end of a 28-mm tube, which supplies fuel and atomizing air to the atomizer. This tube is connected to a vertical traverse to provide translation in the axial direction. The entire axial traversing system is attached to the bottom of the table via a two-dimensional horizontal traverse system. Hence, three degrees of translational freedom are available to the test article. In addition, the fuel tube can be rotated about the axial centerline to any degree of atomizer orientation.

A plexiglass and flexible plastic enclosure surrounds the entire traversing/support system and ensures a stagnant environment by isolating the flowfields studied from room perturbations. This structure also permits seeding of the air entrained by the flowfields, thereby enabling unbiased measurements of the gas phase to be made. Air introduced into the structure is removed via an exhaust system located in the fuel collection plenum. A stainless mesh separates the exhaust entrance from the structure to ensure that the exhaust suction is distributed over the large area of the plenum.

Diagnostics. Measurements of mean and fluctuating velocities for each phase are made using a two-component phase/Doppler system (Aerometrics Model 2100-3). The principle of operation of the instrument has been described in detail elsewhere (Bachalo and Houser, 1984). A schematic of the transmitter and receiver is shown in Fig. 3. The measurement of the size of spheres is based upon a linear relationship between the spatial phase shift of the scattered fringe pattern and the diameter of the scatterer. The velocity is determined from the frequency of the swept fringe pattern. Comparative studies with diffraction (e.g., McDonell et al., 1987; Dodge et al., 1987), visibility (Jackson and Samuelsen, 1987), and extinction (Young and Bachalo, 1987) techniques have demonstrated good size measurement capability. In most cases, the phase/Doppler approach demonstrated advantages over the other techniques.

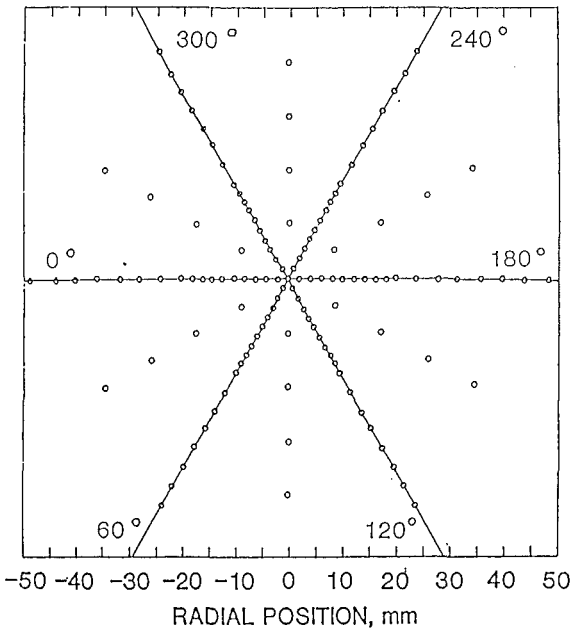

Fig. 4 Measurement locations for each axial station

Discrimination of the continuous and dispersed phases is achieved by sizing all particles, including the seed particles used to track the continuous phase. Al_2O_3 (nominally 1.0 μm) is used to seed the air streams. The seed particles produce size measurements less than 3 μm. Using these scores and those from droplets less than 3 μm in diameter, statistics for the continuous phase are generated. This approach has been applied successfully in previous studies of both monodispersed (e.g., Bluzan, 1988; Mostafa et al., 1988) and polydispersed (e.g., McDonell and Samuelsen, 1988; Rudoff and Bachalo, 1988) flows. In the regions of the flowfield studied in the present work (50 mm and further downstream), particles smaller than 3 μm in diameter track the flow to a good degree.

In addition, the instrument utilizes information from the signals obtained to generate an in-situ measurement of the probe volume cross section. Recent studies have shown that (1) developments in the methods to deduce the sampling cross section have resulted in accurate volume flux calculations in high number density flows (Bachalo et al., 1988), and (2) the values of mass flux correspond in magnitude and trend with those obtained through typical intrusive sampling techniques such as patternation (e.g., McDonell et al., 1987). In the present study, the optical technique alone is used for the volume flux measurement in lieu of a physical probe since the equivalent information is obtained with regard to fuel distributions and, in addition, details are provided with respect to size and velocity distributions. It would not be practical to conduct a detailed mapping such as the one done in the present study if volume flux were the sole quantity sought. In this case, a well-developed patternation system (e.g., McVey et al., 1987) would be more appropriate.

Approach

The approach taken in the current study is to characterize precisely the flowfield produced by a production air-blast atomizer. The first step is to conduct a three-dimensional characterization of the single-phase flow produced by the injector when running the nominal atomization air flow in the absence of fuel. Next, the flowfield with the injected liquid is characterized in the same three-dimensional manner. The two-phase characterization includes the mapping and measurements of statistics for both the liquid and dilute

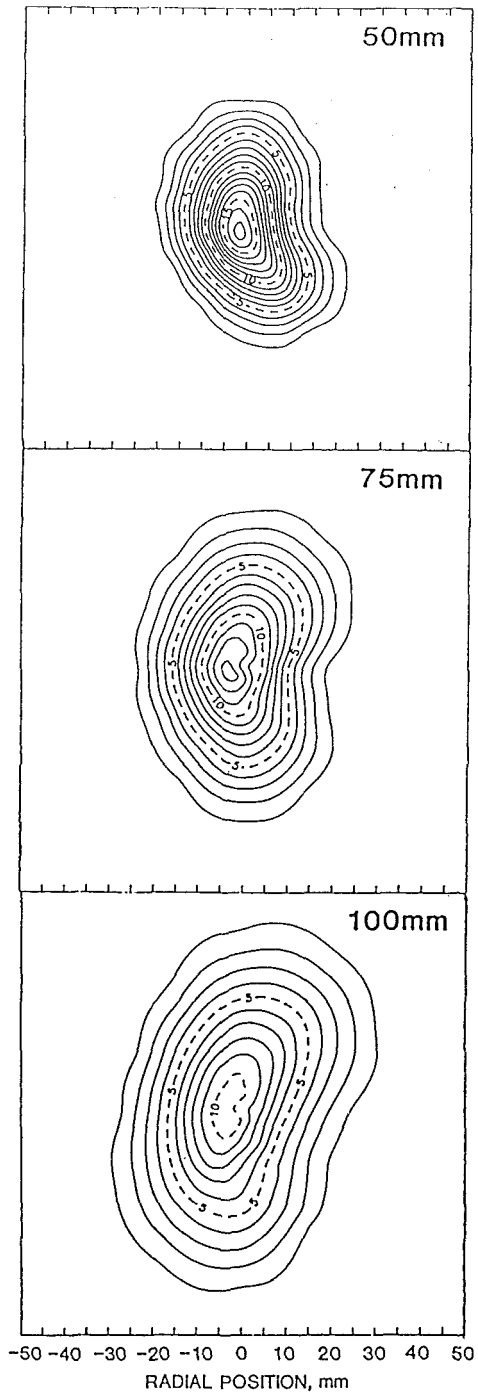

Fig. 5 Isopleths of single-phase axial velocity (m/s)

phase. The trends associated with the single and two-phase flows are then examined in detail to (1) provide understanding of the two-phase interaction and (2) give insight as to the cause and perpetration of asymmetries present in the flow. The characterization consists of measurements of axial and azimuthal velocity for each phase present, and particle size distribution of the dispersed phase, when present. The measurements are conducted at three axial stations (50, 75, and 100 mm), and at six angular orientations of the atomizer (0, 60, 120, 180, 240, and 300 deg) at each axial station. In addition, measurements of partial profiles are conducted at 30 deg increments to ensure adequate coverage of the flowfield. Data are acquired at between 10 and 20 radial stations at each axial station depending on the radial extent of the spray field.

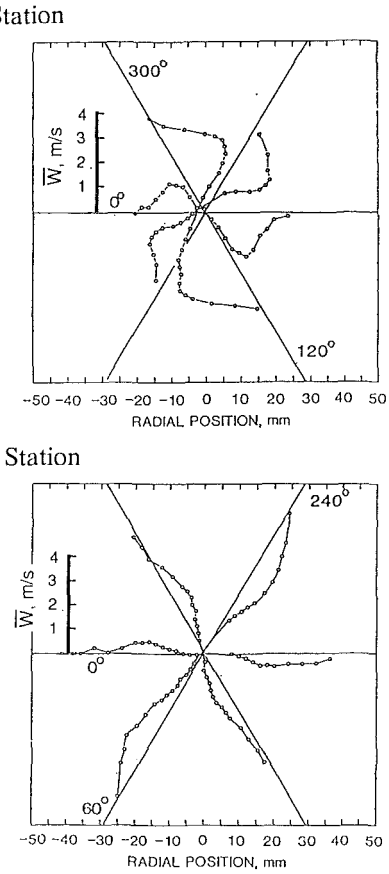

Fig. 6 Single-phase mean azimuthal velocity profiles

Figure 4 shows the locations at which measurements were conducted at each axial station, and provides a reference for the location of each angular orientation.

Results

Results are presented first for the single-phase flow, followed by the continuous phase in the two-phase flow, and finally for the dispersed phase in the two-phase flow. Results are presented in either three dimensions or two dimensions. In the cases where two dimensions are presented, the results are obtained by averaging the data acquired for the six orientations unless explicitly stated as being a profile obtained from a particular orientation.

Symmetry of the Single-Phase Flow. The flowfield symmetry of the atomizer was first characterized in the absence of liquid phase injection to provide a baseline against which to compare the two-phase flow results. Figure 5 shows isopleths of the mean axial velocity at three axial stations: 50, 75, and 100 mm. The plots have an elliptical shape at each location. For the 50-mm case, the major axis of the elliptical shape runs from 300 to 120 deg. The ellipsoidal shape moves through approximately 40 deg of rotation with increasing axial distance. The rotation is due to the azimuthal component of velocity imparted by the swirl vanes in the atomizer.

Figure 6 presents profiles of the mean azimuthal velocity for the six angular orientations of the atomizer studied. Figure 6(*a*) presents the data for the 50-mm axial station. The extension of the ellipsoid is correlated to the presence of an asymmetry in the azimuthal velocity. Note that the azimuthal velocities associated with the 120 and 300 angular orientations are significantly higher. The 0-deg orientation has the least amount of radial spread and it also possesses the lowest

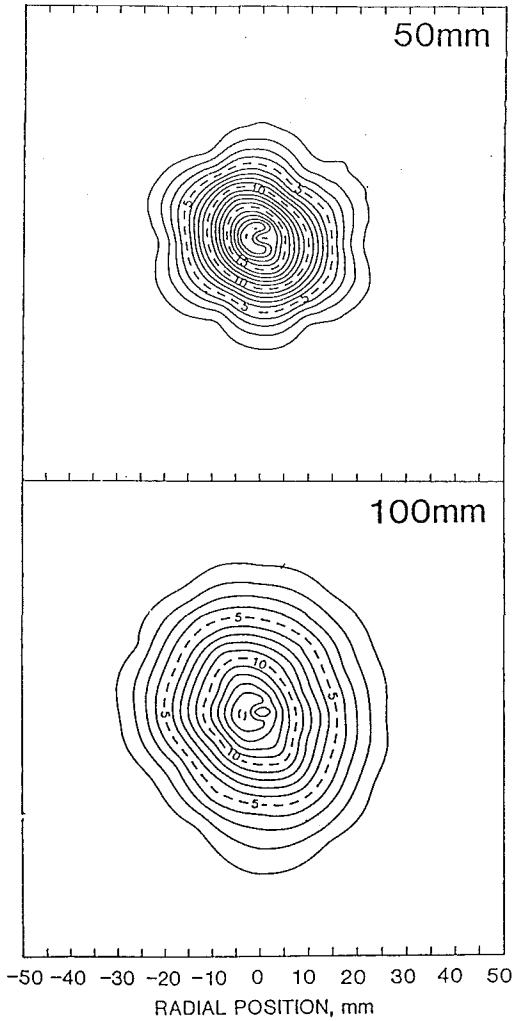

Fig. 7 Isopleths of continuous phase axial velocity (m/s)

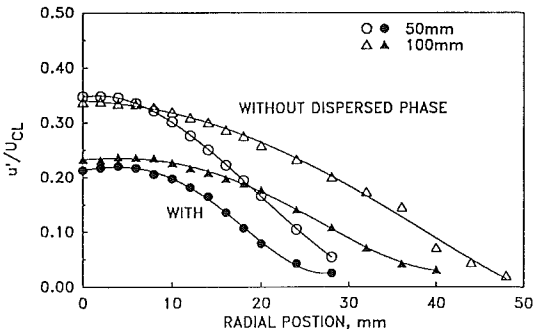

Fig. 8 Continuous phase turbulence intensity

azimuthal velocities. By 100 mm, as shown in Fig. 6(*b*), the local peaks in azimuthal velocity have rotated clockwise to the 240 and 60-deg orientations. Again, the radial spread at these orientations is greater than that at the other orientations. At 100 mm the asymmetry in azimuthal velocity is still noticeable, but is substantially damped out.

Symmetry of the Two-Phase Flow

Continuous Phase. Figure 7 presents isopleths of the mean axial velocity for the continuous phase in the methanol spray field. Note that the presence of the liquid ("dispersed") phase has virtually eliminated the asymmetry present in the single-phase axial velocity field. The flowfield at 50 mm is nearly circular, and the elliptical behavior exhibited by the single-phase flow in the absence of liquid injection is not discernable. Note that the axial velocities associated with the two-phase flow are greater at the centerline region and less at the outer edge, indicating that the presence of the spray increases the gradients in the continuous phase axial velocity.

a) 50 mm Axial Station

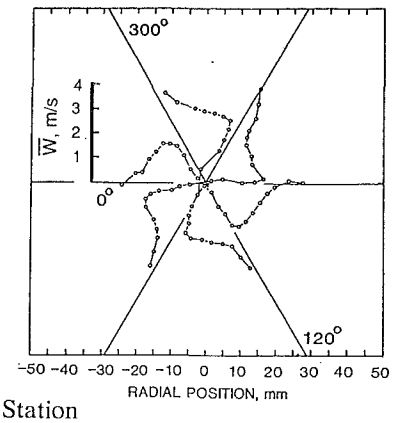

b) 100 mm Axial Station

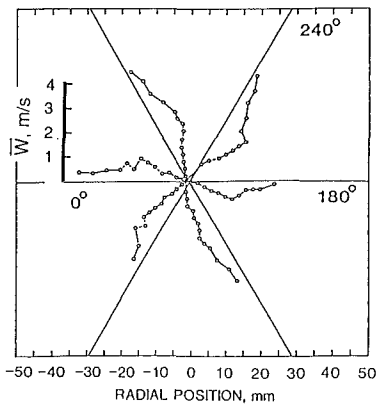

Fig. 9 Continuous phase mean azimuthal velocity profiles

Figure 8 presents radial profiles (averages of each of the seven orientations) of the axial turbulence intensity based upon the centerline value of the mean velocity at each axial station. The presence of the dispersed phase decreases the turbulence intensity of the continuous phase by 30 percent, resulting in decreased velocity decay and spread in the flow.

Figure 9 presents the azimuthal velocity profiles associated with the axial velocity isopleths of Fig. 7. The 50-mm axial station exhibits reasonable symmetry in the azimuthal velocities, a result consistent with the symmetric axial velocity field. However, the azimuthal velocities at 120 and 300 deg are slightly higher, a result that is consistent with the single-phase flow.

The azimuthal velocities at 100 mm are presented in Fig. 9(*b*). Note that the azimuthal velocities for the two-phase flow are slightly greater than the single phase flow at 100 mm (Fig. 6). The swirl is maintained a greater axial distance in the presence of the dispersed phase due to (1) the decrease of turbulence and (2) the momentum transfer between phases (the methanol is injected with swirl, concurrent with the air). At 100 mm, the peak azimuthal velocities occur at 240 deg. and the minimum at 0 and 180 deg orientations, again reflecting results obtained for the single-phase flow. It is noteworthy that the relatively strong azimuthal velocities at 60 deg for the single-phase flow are not present in the two-phase flow, suggesting that the disparity in the two-phase case is affected by

a) 50 mm Axial Station

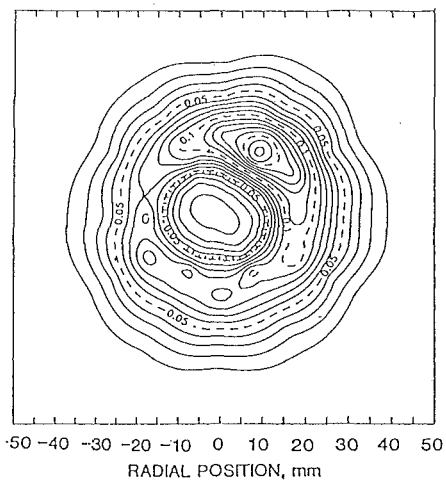

b) 100 mm Axial Station

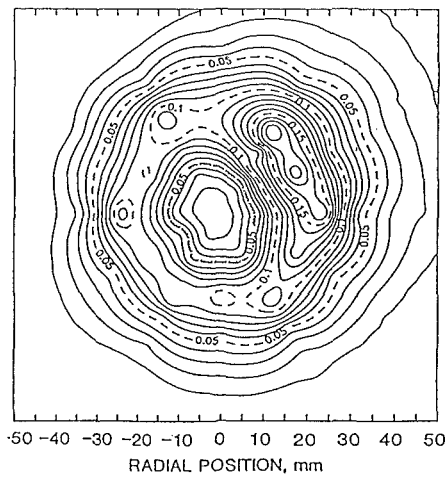

Fig. 10 Isopleths of volume flux (cc/cm^{2}s)

the presence of the dispersed phase. These results demonstrate that, in the present case where equal mass is present each phase, the continuous phase is strongly influenced by the presence of the dispersed phase. One trait that persists from the single to the two-phase flow is the location of peak azimuthal velocities.

Dispersed Phase. Isopleths of the volume flux at the 50 and 100-mm stations are presented in Fig. 10. The hachure marks on the figure indicate the direction of negative gradients. Thus, the contours nearest the centerline are of lower value than those farther from the centerline. The hachure marks in this case indicate that the nozzle is hollow-cone in nature. The results at 50 mm (Fig. 10*a*) show the uniformity in radial spread of the dispersed phase. Note also that the volume flux peaks at the 240-deg orientation. The same results are presented in Fig. 10(*b*) at the 100-mm axial station. By 100 mm, the uniformity in radial spread has degraded. The regions from 120 through 270 deg have considerably more radial spread than do the other regions. The location of the increased radial spread corresponds to the highest value azimuthal velocity profile (240 deg) in both the single and two-phase flows. In addition, the local peak in volume flux has rotated slightly and elongated, showing the rotation and spreading induced by the swirl.

To check the accuracy of the flux measurement, the volume under the contour surface is calculated to provide the total

a) 50 mm Axial Station

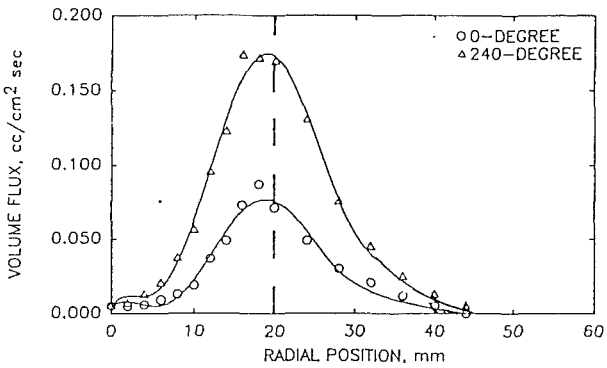

b) 100 mm Axial Station

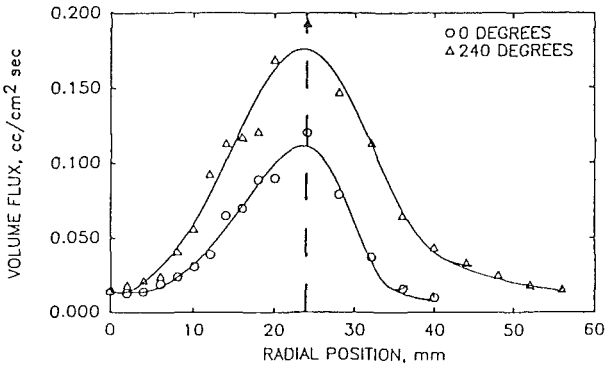

Fig. 11 Radial profiles of volume flux

flow rate at each axial station. At 50 mm, the integrated flow is 30 percent of the measured flow to the atomizer. At 100 mm, it is 93 percent of the measured flow to the atomizer. The value at 100 mm indicates good conservation of mass, especially if evaporation effects are considered. The value at 50 mm, however, does not indicate mass conservation. The possible reasons for this in the present flow are numerous, and include (1) the three dimensionality of the flow, which may lead to erroneous sample area determinations, and (2) relatively high concentration of droplets at the 50-mm station, which leads to erroneous rejection of samples. A smaller sampling volume at 50 mm would likely reduce the error due to the latter reason.

Examination of the 240 and 0-deg Profiles. To understand better the relationship between the phases and the local peak in volume flux, individual profiles are now examined. Results are presented for the 240 and 0-deg orientations, since the greatest disparity in volume flux and radial spread occurs between these orientations. In particular, drop distribution means and drop distributions are examined to understand the volume flux differences better. Additional insight regarding radial spread is also provided by examination of the air/droplet velocity relationships.

Volume Flux. Figures 11(*a*) and 11(*b*) present the individual radial profiles obtained for the volume flux at the orientation of greatest disparity. At 50 mm and 100 mm, the maximum flux occurs for either orientation from between 10 and 30 mm radially. The peak flux occurs at 20 and 24 mm for 50 and 100 mm, respectively. To examine the data with respect to percentage differences, plots of the volume flux at 240 deg divided by the volume flux at 0 deg are presented in Fig. 12. From this figure, the disparity between orientations is clearer.

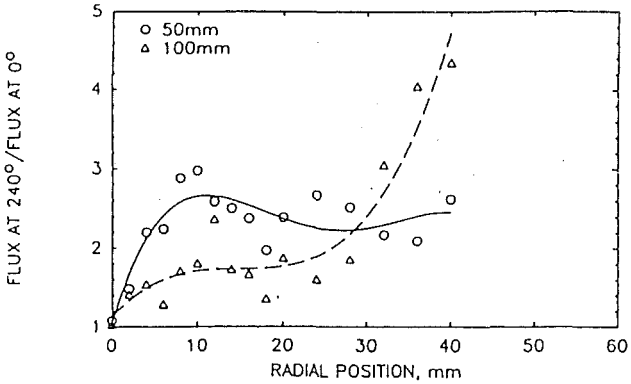

Fig. 12 Ratio of volume flux at 240 deg to volume flux at 0 deg

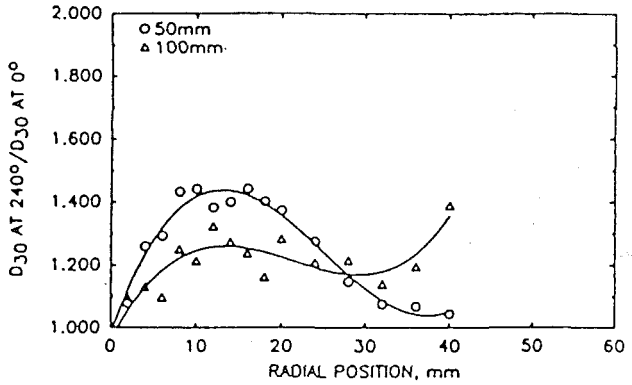

Fig. 13 Ratio of D_{30} at 240 deg to D_{30} at 0 deg

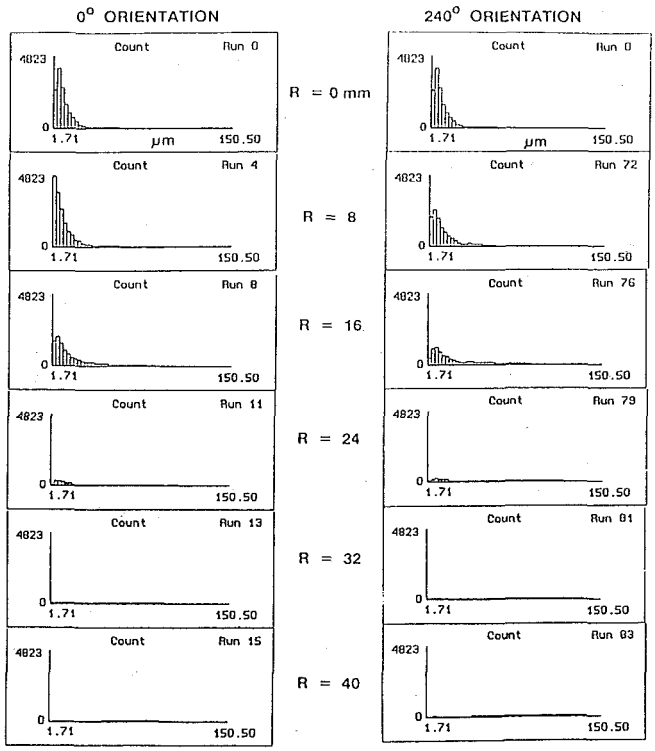

Fig. 14 Normalized droplet size distributions (100 mm)

From two to three times more flux is present at the regions of maximum flux (radial positions between 10 and 30 mm) for 50 mm and from one to two times more at 100 mm. At 100 mm,

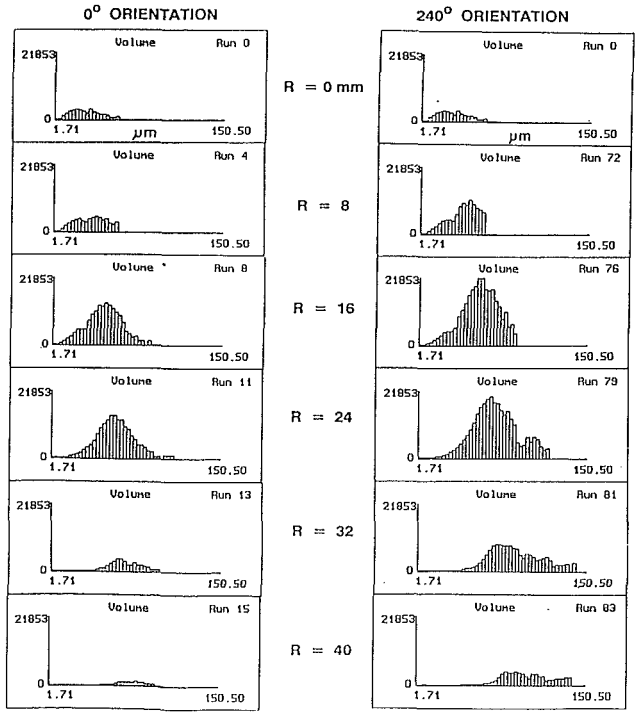

Fig. 15 Normalized droplet volume distributions (100 mm)

the disparity increases beyond 30 mm radially, with up to four times more flux occurring for the 240-deg orientation.

At least two factors affect the volume flux directly: drop size and number of drops. Each of these factors is now examined in order to deduce the importance of each on generating the disparity between these two orientations.

i. Drop Size. In the consideration of disparities in volume flux, the best description of the drop size is the distribution at each point of the volume mean diameter or D_{30}. Radial profiles at 50 and 100 mm of the ratio of the volume mean at the 240-deg orientation to the 0-deg orientation are presented in Fig. 13. At both 50 mm and 100 mm, the discrepancy in the volume mean does not exceed 40 percent at any given radial position. At 50 mm, the distribution volume mean at 240 deg is between 20 and 40 percent higher than that at 0 deg at radial locations corresponding to the greatest volume flux (between 12 and 28 mm). This corresponds to 73 to 173 percent more volume flux at the 240-deg orientation. These differences nearly account for 150 percent greater volume flux at the 240-deg orientation. At 100 mm, the volume mean at the radial locations of greatest flux is 20 to 25 percent higher for the 240-deg orientation, corresponding to 70–95 percent more volume flux. These differences account for the 60 to 80 percent more volume flux on the 240-deg orientation between 12 and 28 mm radially. However, at radial locations beyond 28 mm, the difference in volume mean is not enough to account for the difference in volume flux.

ii. Drop Population. To identify the extent to which various droplet size groups are responsible for the disparity in volume flux, droplet size distributions and droplet volume distributions are presented in Figs. 14 and 15, respectively. The distributions presented are normalized to account for variation in collection time, probe volume area, and system sensitivity as a function of drop size. As a result, the distributions presented reflect identical sensitivity and collection time, and can be used to assess the relative number of drops and volume of drops from point to point.

Figure 14 presents the normalized droplet distributions

a) 0-Degree Orientation

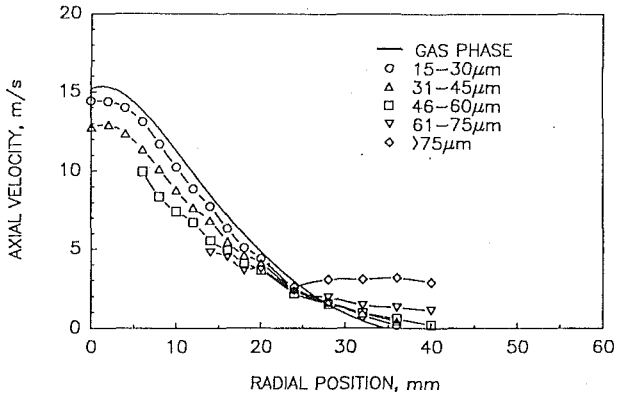

b) 240-Degree Orientation

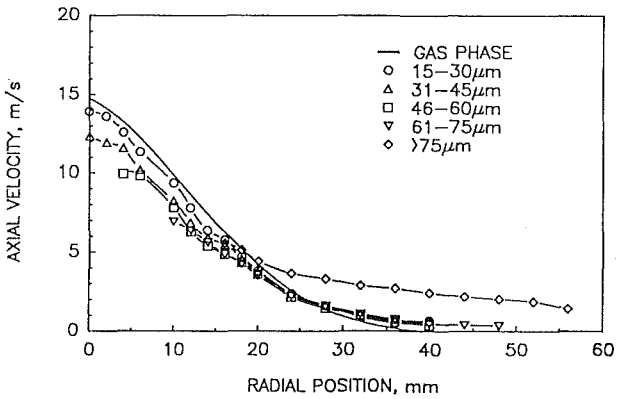

Fig. 16 Gas and droplet velocity profiles (100 mm)

from select radial positions along the 0 and 240-deg orientations. The results show that the greatest population of droplets occurs at the centerline, and that these droplets tend to be small. In the region of greatest dispartity in volume flux (radial positions greater than 16 mm), relatively few drops exist. It is noteworthy that the 0-deg orientation possesses *more* droplets overall than does the 240-deg orientation.

Since the absolute number of droplets may not significantly affect volume flux, the count distributions in Fig. 14 are presented in Fig. 15 as volume distributions. Figure 15 shows that despite the fairly high numbers of small droplets at the centerline, relatively little volume is contributed by these drops. Examination of the volume distributions in the region of greatest volume flux disparity (radial positions greater than 16 mm) indicates that a considerably greater number of large drops are present along the 240-deg orientation. Farther from the centerline, it is observed that the droplets present in this region are large, and that they are considerably larger and more numerous on the 240-deg orientation. This disparity in droplet distribution accounts for the flux differences not explained by the difference in size.

Drop Velocity. Figure 16 presents radial profiles of the gas and droplet mean axial velocities as a function of droplet size. Data are presented at locations where more than 100 drops within the size groupings selected were sampled (10,000 total droplets were sampled at each point). Hence, regions on Fig. 16 where no data are presented for droplets indicate statistically insufficient number of drops of a given size range at that point.

Figure 16 shows that for droplets less than 75 μm in diameter, the profiles for either orientation are similar. The trends for drop size versus axial velocity are consistent, with smaller drops attaining the gas velocity sooner near the centerline. In regions away from the centerline (radial positions greater than 25 mm), the droplets present possess enough momentum to exceed the gas velocity. In these regions, primarily larger drops exist, which (1) have adequate momentum to overcome entrained air and travel away from the centerline, and (2) have the largest influence on the volume flux. The profile for the drops greater than 75 μm on the 240 deg traverse indicate that these drops are responsible for the greater radial spread in volume flux associated with this orientation. Hence, in the present case, the production of larger drops (diameters greater than 75 μm) existing along the 240 deg traverse is responsible for the increased radial spread in volume flux along that orientation.

Little dependency on size exists for the azimuthal component velocity (not presented for brevity); thus it appears that the slightly higher gas azimuthal velocity associated with the 240-deg orientation may also contribute to the increased radial spread. However, decoupling the two effects is not possible without further investigation.

Summary

A precise study of the symmetry of the single and two-phase flow produced by a practical air blast atomizer is conducted using phase/Doppler interferometry. By conducting measurements of two velocity components and drop size distributions for each phase in a three-dimensional manner, the degree of symmetry may be assessed, and the sources of asymmetries may be evaluated.

Conclusions drawn from this study are as follows:

- Two-component phase/Doppler interferometry is capable of distinguishing and measuring statistics for each phase in practical spray fields.
- In the present case, the single-phase flow produced possesses a significant asymmetry, which is considerably damped by the addition of liquid drops in a mass loading of 1.0.
- The addition of the second phase reduces the turbulence and spread of the continuous phase.
- The asymmetry in the volume flux in the present flowfield is mostly due to a disparity in the fuel injection distribution, which is manifested primarily in greater numbers of large drops which have sufficient momentum to travel far from the centerline. Note that the size of the drops alone cannot account for the volume flux disparity.
- Variation in the gas azimuthal velocity field may influence the radial spread of the droplets and causes disparity in radial distribution of the fuel.
- The nature of the asymmetry in azimuthal gas velocity is different in the single and two-phase flows, indicating that, although correlation exists between greater drop radial spread and high azimuthal gas velocities, direct correspondence between the two cases does not exist.
- It is necessary to measure statistics for both phases in two-phase flows to provide the information necessary to understand the transport processes occurring in flows of this type.

Overall, the study demonstrates the complexity of the two-phase interaction and, in addition, shows that the tools necessary to understand the interaction are becoming available. In the present case, the dispersed phase dominates the continuous phase, and is clearly responsible for high local flux at 240 deg. The disparity in radial spread is attributed to both dispersed and continuous phase asymmetry. In cases where air-to-fuel ratios of greater than one are considered, the influence of the continuous phase would become more important. The typical practice of line of sight average drop size, or even of making spatially resolved measurements of drop size, does not provide necessary details regarding phase interaction. Also, steps should be taken to assess symmetry (via patterna-

tion for quick results) before data from a single profile are used to represent the overall behavior of the spray. Without such steps, conducting measurements along a single radial profile at several axial stations within practical flowfields presumes far too ideal a flow.

Acknowledgments

This work was supported, in part, by NASA Contract No. NAS3-24350 (J. D. Holdeman, Contract Monitor) in cooperation with the Allison Gas Turbine Division of General Motors. The participation of Brian Bird in the collection and analysis of the data is gratefully acknowledged. Howard Crum is to be applauded for assistance in the development and maintenance of the facility. Also, the help of Dr. W. D. Bachalo in the specialized development and application of the instrument and software modifications is appreciated.

References

Bachalo, W. D., and Houser, M. J., 1984, "Phase Doppler Spray Analyzer for the Simultaneous Measurement of Droplet Size and Velocity Distributions," *Optical Engineering*, Vol. 23, p. 583.

Bachalo, W. D., Rudoff, R. C., and Brena de la Rosa, A., 1988, "Mass Flux Measurements of a High Number Density Spray System Using the Phase Doppler Particle Analyzer," AIAA Paper No. 88-0236, 25th Aerospace Sciences Meeting, Reno, NV.

Bulzan, D., 1988, "Particle-Laden Weakly Swirling Free Jets: Measurements and Predictions," NASA TM 100881.

Dodge, L. G., Rhodes, D. J., and Reitz, R. D., 1987, "Drop-Size Measurement Techniques for Sprays: Comparison of Malvern Laser-Diffraction and Aerometrics Phase Doppler," *Applied Optics*, Vol. 26, p. 2144.

Jackson, T. A., and Samuelsen, G. S., 1987, "Droplet Sizing Interferometry: A Comparison of the Visibility and Phase Doppler Techniques," *Applied Optics*, Vol. 26, p. 2137.

McDonell, V. G., Cameron, C. D., and Samuelsen, G. S., 1987, "Symmetry Assessment of an Air-Blast Atomizer," AIAA Paper No. 87-2136, 23rd Joint Propulsion Conference, San Diego, California; to appear in the *AIAA Journal of Propulsion*.

McDonell, V. G., and Samuelsen, G. S., 1988, "Evolution of the Two-Phase Flow in the Near Field of Air-Blast Atomizer Under Reacting and Non-reacting Conditions," *Proceedings, Fourth International Symposium on Applications of Laser Anemometry to Fluid Mechanics*, Lisbon, Portugal.

McDonell, V. G., Wood, C. P., and Samuelsen, G. S., 1987, "A Comparison of Spatially Resolved Drop Size and Drop Velocity Measurements in an Isothermal Chamber and a Swirl Stabilized Combustor," *Twenty-First Symposium (International) on Combustion*, pp. 685–694.

McVey, J. B., Russell, S., and Kennedy, J. B., 1987, "High Resolution Patternator for the Characterization of Fuel Sprays," *AIAA Journal of Propulsion*, Vol. 3, p. 202.

Mongia, H. C., and Reider, S. B., 1985, "Allison Combustion Research and Development Activities," AIAA Paper No. 85-1402, 21st Joint Propulsion Conference.

Mostafa, A. A., Mongia, H. C., McDonell, V. G., and Samuelsen, G. S., 1988, "On the Evolution of Particle-Laden Jet Flows: A Theoretical and Experimental Study," to appear in the *AIAA Journal,*.

Rudoff, R. C., and Bachalo, W. D., 1988, "Measurements of Droplet Drag Coefficients in a Polydispersed Turbulent Flow Field," AIAA Paper No. 88-0235, 25th Aerospace Sciences Meeting, Reno, NV.

Young, B. W., and Bachalo, W. D., 1987, "The Direct Comparison of Three In-Flight Droplet Sizing Techniques for Pesticide Spray Research," *Proceedings, International Symposium on Optical Particle Sizing: Theory and Practice*, Rouen, France.